united nations
educational, scientific
and cultural
organization

international atomic
energy agency

the
abdus salam
international centre for theoretical physics

H4.SMR/1150 - 8

Fifth Workshop on Non-Linear Dynamics
and Earthquake Prediction

4 - 22 October 1999

A Model for Complex Aftershock Sequences

A. Correig

Universitat de Barcelona
Dept. Astonomia i Meteorologia
Barcelona, Spain

Submitted to *Journal of Geophysical Research*, 1999.

A model for complex aftershock sequences

Y. Moreno,[1,4] A. M. Correig,[2] J. B. Gómez,[3] A. F. Pacheco,[1]

Abstract

The decay rate of aftershocks is commonly very well described by the modified Omori law, $n(t) \propto t^{-p}$, where $n(t)$ is the number of aftershocks per unit time, t is the time after the main shock, and p is a constant in the range $0.9 < p < 1.5$, and usually close to 1. But there are also more complex aftershock sequences for which the Omori law can be considered only a first approximation. One of this complex aftershock sequences took place in the Eastern Pyrences on February 18, 1996, and was described in detail by *Correig et al.* [1997]. In this paper we propose a dynamic fiber-bundle model to interpret this type of complex aftershock sequences with sudden increases in the rate of aftershock production not directly related to the magnitude of the aftershocks (as in the epidemic-type aftershock sequences). The model is a simple, discrete, stochastic fracture model where the elements (asperities or barriers) break by static fatigue due to subcritical crack growth, and transfer stress according to a local load-sharing rule. We find a very good agreement between the model and the Eastern Pyrenees aftershock sequence and propose that the key mechanism for explaining aftershocks, apart from a time-dependent rock strength, is the presence of dynamic stress fluctuations which constantly reset the initial conditions for the next aftershock in the sequence. These stress fluctuations arise from the highly non-linear function that relates the instantaneous breaking strength with time in the static fatigue law.

[1]Departamento de Física Teórica, Universidad de Zaragoza, 50009 Zaragoza, Spain.

[2]Departament d'Astronomia i Meteorologia, Universitat de Barcelona, E-08028 Barcelona, Spain.

[3]Departamento de Ciencias de la Tierra, Universidad de Zaragoza, 50009 Zaragoza, Spain.

[4]On leave from Departamento de Física, Universidad Tecnológica de la Habana, ISPJAE, Havana 19390, Cuba.

1. Introduction

1.1. The Omori law

Omori discovered scaling in earthquakes in the frequency distribution of aftershocks over one hundred years ago when he proposed a formula to represent the decay of aftershock activity with time [*Omori*, 1894]. Now, hundred years later, it remains as one of the few well established empirical laws in Seismology. As noted by *Utsu* [1995], 'any theory for the origin of aftershocks must explain this law, which is unique for its power law dependence on time'. The Omori law (as modified by *Utsu*, 1961),

$$n(t) = Kt^{-p}, \tag{1}$$

says that the number of aftershocks $n(t)$, measured at time t after the time of the main shock, decays following a power law with exponent p around one ($0.9 < p < 1.5$, with a median of about 1.1, [*Utsu*, 1995]), and K being a proportionality constant. To avoid divergence at $t = 0$, the Omori law is usually written in the form

$$n(t) = K(t + c)^{-p}, \tag{2}$$

where c is an additional 'small' positive constant with dimensions of time (between 0.01 and 1 days, with a median of 0.3 days, [*Utsu*, 1995]) . The power law, scale-free behavior is maintained for $t \gg c$, with a transition to $n(t) = \text{const}$ for $t \leq c$. The cumulative number of aftershocks occurred until time t after the main shock, defined as $\int_0^t n(s)ds$ is

$$N(t) = \begin{cases} K\ln(t/c + 1) & \text{if } p = 1 \\ K\{c^{1-p} - (t + c)^{1-p}\}/(p - 1) & \text{if } p \neq 1 \end{cases} \tag{3}$$

When $p > 1$, $N(t)$ tends to a constant $K/\{(p-1)c^{p-1}\}$ as $t \to \infty$. When $p \leq 1$, $N(t) \to \infty$ as $t \to \infty$.

The Omori law has also been verified in laboratory-scale experiments of brittle rock deformation by measuring acoustic emission [*Scholz*, 1968a,b; *Lockner and Byerlee*, 1977; *Hirata*, 1987; *Sammonds et al.*, 1992]. For a recent review on the role of acoustic emission in Geophysics, see *Lockner* [1993], and references therein. The fulfilment of the Omori law in the scale range from the microscale to the macroscale (more than 8 orders of magnitude in crack size) suggests that a common process is behind the inelastic strain responsible of acoustic emission in laboratory experiments and aftershock sequences in active tectonic faults. But which is this mechanism?

1.2. Physical basis

Benioff [1951] presented the first detailed theory offering an explanation of the causes and characteristics of aftershock sequences in terms of identifiable mechanical properties. According to his theory, aftershocks occur when there is a *time-dependent* recovery of stress following the main shock. The stress recovery was ascribed by Benioff to *creep recovery* of the rocks in the immediate area of the fault.

Since this seminal paper, many laboratory and numerical experiments have confirmed the hypothesis that aftershocks are a process of relaxing stress concentrations produced by the dynamic rupture of the main shock, and that they are, therefore, an intrinsic time-dependent rheological effect [*Scholz*, 1990]. There is, however, no general agreement as for the actual mechanism of stress relaxation, and various hypothesis have been advanced. These can be broadly grouped into two competing schools: the *time-dependent strength* hypothesis, and the *time-dependent friction* hypothesis. The time-dependent strength hypothesis started with the aforementioned paper by *Benioff* [1951], and the time-dependent friction hypothesis has its origins in *Brace and Byerlee*'s [1966] suggestion that earthquakes are a sort of stick-slip phenomenon controlled by friction between the two sides of a fault.

The first time-dependent friction model of aftershocks was proposed by *Dieterich* [1972b] using a modified 1-dimensional Burridge-Knopoff fault analogue [*Burridge and Knopoff*, 1967], with a combination of viscoelastic response and time-dependent friction. Because viscoelastic recovery can only partially restore the stress drop that occur during an earthquake, it is necessary to employ a mechanism whereby the fault will be weaker following an earthquake than it was prior to the earthquake. A laboratory basis for this weakening is provided by the time-dependent friction observations of *Dieterich* [1972a] and subsequent generalizations of this concept that run under the name of rate- and state-dependent friction laws [*Dieterich*, 1979; *Ruina*, 1983; *Rice and Ruina*, 1983; *Gu et al.*, 1984; *Rice and Tse*, 1986; *Cochard and Madariaga*, 1996; *Wennerberg and Sharp*, 1997]. Recently, *Dieterich* [1994] formulated a continuous model for the rate of earthquake production in terms of a general non-linear friction law, assuming also that the earthquake rate is due to the elastic stress change associated to prior earthquakes. He derived two general equations for the earthquake (aftershock) rate following a stress step, both compatible with the mod-

ified Omori law, Eq. (2), at least in some temporal range.

On the other hand, *Scholz* [1968b] formulated the first time-dependent strength model of aftershocks. He suggested that a time-dependent strength of the rocks in the area of the main shock could be the cause of the aftershock sequences and invoked *static fatigue* due to local overloads to stresses much higher than their long-term strength as the main mechanism of aftershocks. Based on *Scholz*'s [1968a] laboratory experiments on static fatigue of quartz, *Das and Scholz* [1981] formulated a general model of aftershocks based on the theory of elastic fracture mechanics and the concept of *subcritical crack growth* [*Atkinson*, 1984]. They showed that this model is consistent with the decay rate of aftershocks as expressed by the Omori law, and that is able to reproduce many other characteristics of real aftershock sequences. More recent works and papers that stress the role of time-dependent strength in aftershock dynamics are: *Yamashita and Knopoff* [1987], who assume that stress corrosion is the physical mechanism for the delayed fracture in aftershocks; *Marcellini* [1995, 1997], advocating static fatigue, together with stress inhomogeneities, as the cause of Omori-law aftershock sequences; and *Lee* [1999] and *Lee and Sornette* [1999], who constructed a fuse network model of aftershocks incorporating a time dependent strength compatible with the mechanism of subcritical crack growth. All these models of aftershocks also obey the Omori law.

Static fatigue, also known as stress-, creep-, or delayed fracture is the basic way of time-dependent failure under constant load of a broad variety of materials, including textile fibers [*Coleman*, 1957], fiber composites [*Phoenix*, 1977], wood [*Garcimartín et al.*, 1997], microcrystals [*Pauchard and Meunier*, 1993], gels [*Bonn et al.*, 1998], policrystalline ceramics [*Deuerler et al.*, 1985], metals [*Williams*, 1973], silicate glasses [*Charles*, 1958], minerals [*Scholz*, 1968a; *Barnett and Kerrich*, 1980], and rocks [*Atkinson*, 1984]. In all these cases, the signature of static fatigue is the observation of a failure strength that is a function of the load history of the material. The physical mechanism of static fatigue depends both on the material and the environmental conditions. For *brittle* materials, and from the point of view of fracture mechanics, time-dependent strength is commonly associated with *kinetic fracture*, *i.e.*, with the propagation of cracks under a crack tip stress intensity factor below the modulus of cohesion of the material [*Kostrov et al.*, 1969]. This propagation is stable and quasi-static, and is referred to as subcritical crack growth, where 'quasi-static' means at velocities much less than the sonic velocity of the medium [*Das and Scholz* , 1991].

Material break down according to two different scenarios. In the first one, which is typical of pure crystals, there is no or little damage up to the rupture, which occurs suddenly. In the second scenario, typical of highly heterogeneous media, the system is progressively damage, first in an uncorrelated manner and then, as strain increases, the damage becomes more and more localized, with crack coalescence announcing the incipient macroscopic fracture. Rocks under brittle conditions (i.e., in the seismogenic zone of the earth crust, where earthquakes nucleate) belong to this second type of material, highly heterogeneous, which develop a pervasive population of microcracks, termed Griffith flaws, that grow subcritically and are responsible of the time-dependent strength of the earth crust. The presence of a chemically active fluid environment saturating the pore and crack space enhances this subcritical crack growth, a mechanism known as *stress corrosion* [*Charles*, 1958; *Wiederhorn*, 1967]. There is ample evidence that geological materials under brittle conditions own their time-dependent strength to the mechanism of subcritical crack growth assisted by stress corrosion [*Atkinson*, 1984; *Atkinson and Meredith*, 1987].

In this paper we take the perspective of the time-dependent strength school and propose a discrete fracture model to describe complex aftershock sequences based on the concept of static fatigue by subcritical crack growth, and where stress fluctuations among the elements in the system (to be identified with barriers or asperities in the 'dynamic' sense of *Cochard and Madariaga* [1996]) play a fundamental role in explaining the production rate of aftershocks.

1.3. Deviations from the Omori law

As mentioned above, the Omori-law decay rate of aftershocks following a main shock is an almost universal characteristic of seismicity (as compared to the more irregular patterns of premonitory activity as foreshocks or quiescence). But despite this universality, many real aftershock sequences display anomalies in the decay rate that depart from the simple Omori-law behavior. Among these anomalies we can cite [*Utsu*, 1995]: (i) cases in which seismic activity following the main shock can not be represented by a simple power law due to mixing of different series of activity; and (ii) cases where aftershocks decay, as a

whole, according to the Omori law, but depart temporarily from the formula due to abrupt changes in activity (accelerations and/or quiescence).

In this paper we are interested in aftershocks series that do not follow rigorously the Omori law, and in particular in this second type of anomalies where sudden accelerations in the rate of aftershock activity are not directly linked to aftershocks of bigger magnitude. This last case is the so-called epidemic-type aftershock sequence, ETAS, where each aftershock has its own sequence of aftershocks [*Ogata,* 1988], and can be thought of as a fractal version of the simple Omori relaxation formula. There are, however, some aftershock sequences where the changes in decay rate are *independent* of the magnitude of the aftershocks that provoke these changes in activity, and that can not be ascribed to the ETAS model. One of this aftershock sequences took place in the eastern Pyrenees on February 18, 1996 [*Correig et al.,* 1997] and in this paper we propose a dynamic (static fatigue) fiber-bundle numerical model as a framework to interpret this type of aftershock sequences.

1.4. Fiber-bundle models

Fiber-bundle models (FBM) are simple discrete stochastic fracture models amenable to either close analytical or fast numerical solution, which arose in intimate connection with the strength of bundles of textile fibers [*Daniels,* 1945; *Coleman,* 1957]. Since Daniels' and Coleman's seminal works there has been a long tradition in the use of these simple models to analyze failure of heterogeneous materials (*Vazquez-Prada et al.*, [1999] and references therein).

FBM come in two 'flavors', static and dynamic. The static versions of FBM simulate the failure of materials by quasistatic loading, i.e., by a steady increase in the load over the system up to its macroscopic failure. Time plays no role in these models, load is the independent variable, and the strength of each element is considered to be an independent identically distributed random variable. On the other hand the dynamic FBM simulate failure by stress-rupture, creep-rupture, static-fatigue or delayed-rupture, i.e., a (usually) constant load is imposed over the system and the elements break by fatigue after a period of time, known as the *lifetime* or *time-to-failure* of the element. Time acts as the independent variable, and the lifetime of each element is an independent identically distributed random quantity. In this paper we are only interested in the dynamic fiber-bundle models, as aftershocks are an intrinsic time-dependent phenomenon.

Three are the basic ingredients common to all FBM: (*i*) a discrete set of N elements located on the sites of a d-dimensional lattice; (*ii*) a probability distribution for the failure of individual elements; and (*iii*) a load-transfer rule which determines how the load carried by a failed element is to be distributed among the surviving elements in the set. For the aftershock model we use a 2-dimensional square lattice of L^2 elements, where L is the size of a side of the square, a Weibull-type probability distribution, and a local load transfer mechanism among the elements in the lattice.

This paper is organized as follows: in Section 2 we briefly summarize the characteristics of the aftershock sequence of the Eastern Pyrenees, described in detail by *Correig et al.* [1997]; Section 3 is devoted to the presentation of the particular dynamic FBM used to simulate the aftershock sequence; it is a discrete, two-dimensional, local version of the FBM where the elements break by static fatigue. Finally, Section 4 presents the main results obtained from the model, the comparison of these results with the real aftershock sequence, and our conclusions.

2. The data

On February 18, 1996, a local magnitude $M_L = 5.2$ earthquake occurred in the Eastern Pyrenees, with epicentral location N42°47.71', E2°32.30' and focal depth of 8 km [*Rigo et al.,* 1997].

The series of aftershocks that followed this event was recorded at the three-component continuous broadband seismic station at the Tunel del Cadí, located at about 80 km SW of the epicentral area. Altogether, the series consists of 337 event (complete for a threshold magnitude of 1.9), spanning 1846 hours (77 days) from the time of the main shock, and with magnitudes ranging from 1.9 to 3.8. Figure 1a shows the cumulative series of aftershocks, along with the magnitude of the events. The sudden change in slope at about 300 hours is not due to incompleteness of the series, and from the point of view of the magnitude of the aftershocks, there is no specific characteristic, nor any relevant event, that justifies this sudden change in the event rate. Because of this different behavior, we will restrict our attention to the series defined by the first 300 hours, with a total of 308 events, as displayed in Figure 1b.

The most striking feature of this series is the change in concavity of the cumulative curve not cor-

related with any significant event (as it would be the case from the point of view of a ETAS model), suggesting an increase in the rate of aftershocks production apparently not related to any relaxation process. If we try to fit Fig. 1b to Eq. (3), no unique set of parameter is able to fit the entire range and, furthermore, the values of p so obtained are abnormally low (0.56 for the 0-100 hours interval, and 0.64 for the 140-300 hours interval). The fit and the value of p do not improve if the magnitude threshold is increased [*Correig et al.*, 1997].

The interpretation of the Omori law as a relaxation process suggests a way of separating the aftershocks in the series into two classes: class A for the events that follow a relaxation law and class B for those events that do not. The criterion to assign the events to classes A or B is the following: if the interval of time Δt_i between events i and $i-1$ is strictly larger than the interval of time Δt_{i-1} between events $i-1$ and $i-2$, the event i belongs to class A; otherwise it belongs to class B. Events belonging to class A are termed *leading aftershocks*, and those belonging to class B, *cascades*. Figure 1c shows the aftershock sequence classified as leading events (solid circles) and cascades (dots). Note that a cascade is initiated by a leading aftershock and that this leading aftershock has no significative different magnitude.

The fit of Eq. (3) to the series formed by the leading aftershocks is shown in Fig. 2a. The fit has improved notoriously from the initial fit to the whole sequence, and the value obtained for the exponent is now $p = 0.94$, much more in agreement with the standard values for worldwide aftershock sequences. Figure 2b depicts the series of cascades, in which the first term of each cascade is a leading aftershock. Two important features are readily visible from the figure: (*i*) the cascades are in general well approximated by straight lines; and (*ii*) their corresponding slopes decrease with time. A plot of the slope s of the cascades against time t (Figure 3) shows the remarkable fact that there exists a power-law relationship of the form $s \propto t^{-\nu}$ between them, with $\nu \approx 0.71$.

The properties summarized in Figs. 1 through 3 for the aftershock sequence of the Eastern Pyrenees can be described at first order with the modified Omori law, Eqs. (2) and (3). But at second order there are important non-random fluctuations about this law (represented by the cascades) that can not be fitted in detail with, nor accounted for, the Omori law and its relaxation origin. In the next Section we will construct a model that is able to account for this second order deviations from the Omori law, and for the Omori law itself, of course.

We want to stress here that the characteristics of the series of aftershocks from the February 18, 1996, Pyrenees mainshock are by no means 'exceptional'. On the contrary, they seem to be a rather general feature of aftershock series. The authors are currently analyzing various aftershock sequences (Greece, Kobe, Landers, Northridge) and have found a behavior very similar to that of the Pyrenees aftershock sequence. Results will be reported elsewhere.

3. The model

3.1 Background

In engineering and geophysics, the failure of an heterogeneous material is generally modeled in terms of a statistical distribution of lifetimes when subject to an applied stress σ_0. In a discrete model consisting of a set of N elements (to be identified with asperities or barriers on a fault plane), the failure of each element is sensitive to both the elapsed time and its stress history (precisely, this dependence on the stress history is what makes intractable the formulation and resolution of fully-grown continuous deterministic dynamical models of fracture). In this context, we can express the probability $P(t;\sigma(t))$ of a single element i failing at time $t_{i,0}$ after suffering the load history $\sigma_i(t)$ as [*Coleman*, 1957]

$$P(t_{i,0};\sigma_i(t)) = 1 - \exp\left\{-\int_0^{t_{i,0}} \kappa\left(\sigma_i(t)\right) dt\right\}, \quad (4)$$

where $\kappa(\sigma)$ is the hazard rate or breaking rule (number of failures per unit of time). The hazard rate is commonly expressed in the form

$$\kappa(\sigma) = \nu_0 \left(\frac{\sigma}{\sigma_0}\right)^{\rho}, \quad (5)$$

which has both experimental [*Coleman*, 1958] and theoretical [*Phoenix and Tierney*, 1983] support, and is compatible with subcritical crack growth equations, as will be discussed in Section 4 . Here, ν_0 is the hazard rate under the reference load σ_0, and ρ is a constant, usually in the range $2 < \rho < 50$, thus conferring a highly nonlinear form to the equation.

For constant load, inserting Eq.(5) into Eq.(4) gives

$$P(ti,0;\sigma_i) = 1 - \exp\left\{-\nu_0 \left(\frac{\sigma_i}{\sigma_0}\right)^{\rho} t_{i,0}\right\}. \quad (6)$$

This equation has the form of a Weibull probability distribution function, which is widely used in engineering. The widespread use of Weibull statistics stems from the experimental fact that real materials follow very closely Weibull probability distribution functions for both the strength and the time-to-failure of the individual elements [*Daniels,* 1945; *Coleman,* 1957, 1958; *Phoenix and Tierney,* 1983; *Okoroafor and Hill,* 1995].

Once asperities in the fault plane begin to fail, stresses are no longer homogeneous. Under these circumstances, the stress history of a particular asperity could be extremely complicated, even more if healing of previously broken asperities is allowed. In order to accommodate the increase in stress caused by local stress redistribution from failed asperities, a *reduced time to failure* $T_{i,f}$ is introduced [*Newman et al.,* 1995; *Gómez et al.,* 1998]:

$$t_{i,0} = \int_0^{T_{i,f}} \nu_0 \left(\frac{\sigma_i(t)}{\sigma_0} \right)^{\rho} dt. \qquad (7)$$

In the case of independent elements (*i.e.*, no stress transfer), $\sigma(t) = \sigma_0$ and $t_{i,0} = T_{i,f}$ for all elements $i = 1, ..., N$. When stress redistribution between elements is permitted, the actual time to failure of element i, namely $T_{i,f}$, is reduced below $t_{i,0}$ if stress is transferred to that element. The time $T_{i,f}$ is obtained by requiring that Eq. (7) is satisfied. In this way we are able to take into account, at the same time, the intrinsic time-dependent strength of asperities, Eq. (6), and the additional reduction in its lifetime due to stress transfer between failed and unfailed elements, as given by Eq. (7). Notice that this stress transfer is dynamic, and is equivalent to a resetting of initial conditions for continuous models of earthquakes.

The stress history for a particular element k is made of steps. Let asperity k be supporting a stress σ_k^0 at time t_0. It will continue to support σ_k^0 until a stress transfer from one of the nearest neighbors occurs. In this moment, say t_1, asperity k instantaneously changes its load to $\sigma_k^1 = \sigma_k^0 + \sigma_{nn}$, where σ_{nn} is the stress transferred by the neighboring element. Then, in a later time t_2, asperity k could receive again load from another neighbor, suffering a second step-like increase in stress. Put into symbols, the stress history of elemet k can we written as

$$\sigma_k(t) = \begin{cases} \sigma_k^0 & \text{for } t_0 \le t < t_1 \\ \sigma_k^1 & \text{for } t_1 \le t < t_2 \\ \sigma_k^2 & \text{for } t \ge t_2. \end{cases} \qquad (8)$$

This step-like stress history continues until asperity k fails by static fatigue at the time $T_{i,f}$, Eq. (7).

3.2 Probabilistic approach

These models can be solved by a Monte Carlo technique as explained in detail in *Newman et al.* [1995]. In *Vazquez-Prada et al.* [1999], however, we have devised an alternative approach to dynamic fiber-bundle models; it is particularly clarifying and intuitive. We call it the *probabilistic approach* and will be applied to this model of aftershocks.

From a probabilistic point of view, for a given distribution of stress σ_i, $1 < i < N$, the time interval δ for one asperity to break is

$$\delta = \frac{1}{\sum_{i=1}^{N} \kappa(\sigma_i(t))}, \qquad (9)$$

where $\kappa(\sigma)$ is given by Eq. (5). For the sake of simplicity, we will assume from now on that $\nu_0 = \sigma_0 = 1$, so that we can rewrite Eq. (9) as

$$\delta = \frac{1}{\sum_{i=1}^{N} \sigma_i^{\rho}}, \qquad (10)$$

and the probability that precisely asperity k is the affected one is

$$p_k = \delta \kappa(\sigma_k) = \delta \sigma_k^{\rho}. \qquad (11)$$

The initial values of σ_i will be taken from a uniform probability distribution ($0 < \sigma_i < 1; 1 \le i \le N$). This would represent the dynamical state of the fault just after the main shock. Besides, we will introduce *dissipation* in the model. This is quantified by a constant factor $0 \le \pi \le 1$. When an element breaks, π times its stress is distributed among the elements occupying the nearest neighboring positions, and $(1 - \pi)\sigma$ is lost. The introduction of dissipation is necessary to describe a global progressive relaxation process in the system. We will suppose open borders, so that stress is also lost through the boundaries. Note that, in the model, once an element breaks it remains inactive until it receives load again, being a possible mechanism for this process a healing phase [*Heaton,* 1990; *Cochard and Madariaga,* 1994].

Due to the dissipation, the total stress in the system, S, systematically decreases. If the value $\rho = 1$ were considered, then from Eq. (10), the successive δs would necessarily be longer and longer. But ρ is bigger that one, and this is the reason why one can have a step down in S and find a shorter value of δ.

This is the key point to understand our model. In the general trend of S reduction and hence temporal deceleration, the stress transfers in the system provoke local inhomogeneities in σ, and due to the high values of ρ, this leads to temporal accelerations. These accelerations are embedded in the general trend of power-law relaxation. This model leads to the fulfilment of Omori's law, as can be checked in the next Section, because it is analogous to a mechanism of stress corrosion in which aftershock events are triggered each time the strength threshold decays below the local stresses [*Lee and Sornette,* 1999].

To reinforce the appearance of the sudden accelerations, we will implement the following three rules:

(*i*) when, due to stress fluctuations, σ in a site i surpasses the value of 1, then the element that breaks is necessarily that one. The δ for that breaking is obtained by applying Eq. (10), but, in this case that is equivalent to stating that $p_i = 1$, $p_{j\neq i} = 0$. If ρ is big enough, Eq. (11) leads to the same result because p_i would be considerably bigger than the others.

(*ii*) when σ_i becomes bigger than 1, we say that an avalanche has started. The avalanche ends when all the sites in the system have σ values lower than 1. During an avalanche, which will involve several δs, all the elements that have surpassed, at any step of the avalanche, the condition $\sigma > 1$ remain inactive with $\sigma = 0$ until the end of the avalanche. This is introduced in order to increase the local stress accumulations, which lead to shorten the corresponding value of δ. This assumption is reasonable because in very short δ there would not be time for healing. And

(*iii*) If during an avalanche step, there are several elements with $\sigma > 1$, the δ will be calculated, as ever, using Eq. (10), but all the elements with stress surpassing the threshold decay simultaneously in that step.

As a resume, we observe that in the process of relaxation of the system there are normal events and avalanche events. The former refers to the failure of one element when no element in the system has $\sigma > 1$. The latter corresponds to the failure of one element (or several) with $\sigma > 1$. Eq. (10) is always used for the calculation of the time intervals. Typically the δs in the avalanches are shorter because of the large stress concentrations induced by rule *ii)*, and the magnitude of the exponent ρ. With these rules, it is obvious that the avalanches become extinct with time because as S declines, it is more difficult to locally accumulate load as to surpass the unity.

The running of the model proceeds as follows. First, we load each element in the square lattice with a random initial stress σ_i, $i = 1, ..., N$, taken from a uniform probability distribution $0 \leq \sigma_i < 1$. Then, we calculate the δ or time interval until the next failure by using Eq. (10). Now, we check if all the elements have their σ-value lower than one. If this is the case, the rupture corresponds to a normal event, so we apply Eq. (11) to find out which element is going to break. This is done by generating a random number between 0 and 1, and comparing it with p_k. This points to a specific element that fails and transfers the load it bears to its nearest neighbors. During the transference which we consider as instantaneous (*i.e.*, step-like), there is dissipation, i.e., the fraction $(1-\pi)\sigma$ is removed from the system. The second case corresponds to the situation in which an element (or several elements) supports a load bigger than one. In these cases, those elements break following rules (*i*), (*ii*) and (*iii*) and the load is transferred as before. The simulation is carried out until a minimum value for the total load in the system is reached (here, we have imposed that the load accumulated in the whole system must be larger than 10^{-14}). This is a kind of alternative to mimic the real threshold detection magnitude of seismograms or the background seismicity.

One ending comment is in order. We have started from a randomly distributed load configuration in the system; our two main results, i.e., the general trend of relaxation, fulfilling Omori's law, and the observation of sudden accelerations produced by the load dynamical fluctuations, are not affected by this assumption.

4. Results and Conclusions

We have carried out numerical simulations which show the fulfilment of Omori's law and which reproduce the features already commented, that is, a cumulative plot with sudden variations in the number of events (accelerations). We show here the results for a two-dimensional system of 50×50 elements located on a square lattice, with ρ equal to 30 and a conservation level of $\pi = 0.7$. Other simulations have also been performed varying the size of the system, the value of ρ and the conservation level, π. We have found that the results are indeed very close to those exposed here with equal qualitative behaviour. Nevertheless, it should be noted that although the results are robust over a large range of parameters, different characteristics arise for extreme values of ρ and π.

Figure 4 shows the rate of aftershocks dN/dt as a

function of time. Time is represented in dimensionless units and it is the sum of the successive δs. The straight line has a slope of -1.01 ± 0.02. Thus, the $1/t$ decay is confirmed and is in full agreement with Omori's law for real aftershock sequences. The power law depicted is very robust over a wide range of the parameters that characterize the model. The most critical parameter is the conservation level since for values of π close to unity, the system does not dissipate enough as to avoid its complete failure. Besides, for large dissipation $\pi \ll 1$, the power law extends only to a few decades, and the number of decades decreases as π decreases. Nevertheless, in all cases the exponent of the power law decay is very close to unity. The major vertical spikes of Fig. 4 correspond to avalanche-type events that disappear as time goes. The smaller fluctuations for large times reflect the intrinsic probabilistic nature of the model and is not related at all to the appearance of avalanches. This is clearly seen in Fig. 5 where we have plotted the cumulative number of aftershocks versus time instead of the differential plot of Fig. 4. As can be observed in Fig. 5, sudden accelerations appear in the first stages of rupture. This behavior resembles very well that previously reported in Sec. 2 for the eastern Pyrenees aftershock sequence (see Fig. 1).

In our model, the changes in aftershock rate are related to the readjustments of local stresses when events take place. During the first stages of failure, the elements (asperities) are broken, in general, one by one, and no local accumulations of load are likely to occur. As time goes, local concentrations of stress appear in the system and there is a high probability of finding a fault region in which the load supported by the elements is close to the threshold value $\sigma = 1$. That is, there is a large heterogeneous stress state in which one failure will trigger an avalanche. During the evolution of the avalanche the local accumulation of load increases. This fact together with the high value of ρ, provokes that the δs corresponding to this stage of rupture are considerably reduced. As a result, we observe the step-like change in the cumulative number of events. Finally, the avalanches disappear for large times since we are dealing with a non-conservative model and then it would be unlikely to accumulate stress in local regions as to surpass the value $\sigma = 1$, since the total load in the system systematically decreases.

It is of interest the further investigation of the acceleration events in order to get additional insight about the observed aftershock sequences. One simple way for doing that was already explained in Sec. 2. It consists of decomposing the original series of aftershocks in leading events and cascades depending on whether a relaxation law is accomplished or not. We have followed the same procedure with the synthetic data. The series of cascades obtained in such a way is shown in Fig. 6. Part (a) shows the series after removing all the cascades, i.e., leaving only leading aftershocks, and in Fig. 6b we plot the cascades, in which the first event of each cascade is a leading aftershock. The decomposition obtained from the model is indeed indistinguishable of that corresponding to the real series of events (Fig. 2). Two characteristics of the series of cascades are again relevant: one, the elapsed time between successive leading events is larger than the preceding one in complete agreement with the supposition of a relaxation process, and second, the series of cascades can be well approximated by straight lines whose slopes decrease as time passes. This later characteristic could be used to quantify the observed jumps in the cumulative plot of aftershocks and to explain why they are present mainly in the first stages of rupture. The larger jumps are related with the occurrence of avalanches, which are caused by local accumulations of stress; so it is expected that when avalanches disappear due to dissipation, the changes in the rate of occurrence are more spaced in time as well as that the cascades consists of fewer events. Of course, there will be fluctuations about the power law trend even in case that avalanches have deceased. Thus, we expect slope values gradually closer to zero as time tends to infinity. This is clearly appreciated in Fig. 7, where we have represented in a log-log plot, the slopes of the cascades versus the occurrence time of the leading event that initiate each cascade. As for the observed series of aftershocks, the slopes fit very well a power law with an exponent of about 1.08. Thus, the qualitative behaviour is again captured. The discrepancy between the slopes is not surprising since the simplicity of the model as compared with the inherent complexity of the real phenomenon we want to resemble. The reason of this particular behavior, that is, why the slopes follow a power law and no other law, is unclear for us up to now.

As we advanced in Sec. 3, the power law hazard rate, Eq. (5), has been used to fit experimental results of time-to-failure on various materials [*Coleman,* 1957; *Phoenix,* 1977]. Besides, *Phoenix and Tierney* [1983] derived it from a kinetic theory of thermaly activated atomic bond rupture [*Zhurkov,* 1965],

and showed that in many circumstances it is a better approximation than the exponential breaking rule, $\kappa(\sigma) = \alpha \exp(\beta\sigma)$, also used in modeling time dependent fracture [*Coleman*, 1957].

Equation (5) has the same form as Charles power-law to describe stress corrosion induced subcritical crack growth in geological materials [*Atkinson*, 1984]:

$$v = v_0 \exp(-H/RT) K_I^n, \tag{12}$$

where v is the crack velocity, H is the activation energy, R is the gas constant, T is the absolute temperature, K_I is the stress intensity factor for mode I fracture, and v_0 and n are constants. Sometimes, n is known as the stress corrosion index. Nominal values at room temperature and in wet rock are [*Atkinson and Meredith*, 1987]: 15-40 for quartz and quartz rocks; 10-30 for calcite rocks; 30-70 for granitic rocks; and 25-50 for gabbro and basalt. If we assume constant temperature, Eq. (12) can be simplified to

$$v = A K_I^n, \tag{13}$$

which is identical to Eq. (5) if we substitute σ by K and identify the breaking rate expressed by Eq. (5) with the crack opening velocity expressed by Eq. (13).

Summarizing, we have proposed a discrete, dissipating, stochastic model to explain the appearance of sudden accelerations in an anomalous series of aftershocks. The approach presented here models the complex series of aftershocks as a sequence of failure of asperities on a fault plane. The stressing history and the existence of a stress threshold determine the timing of events in the series. The changes in the rate of occurrence can be explained in terms of the heterogeneities generated by the probabilistic dynamical rules of the model. The asperities break at a time given by their stress history and transfer their load to their neighborhood. This yields a state where regions of relative large stress concentrations appear through the fault. Then, when a failure occurs in one of those regions several asperities are stressed enough as to surpass the unity triggering an avalanche, and then the subsequent increase of local activity is translated into an increase in the event rate. In this way, the model captures the fundamental role of the stress history which result in that relative modest transfers of stress provoke very large perturbations in the aftershocks activity which cease when the excess of stress is completely released.

We have found a very good agreement between the model and the observed aftershocks sequence. The rate of aftershocks decay follows a power law with exponent very close to unity decorated by fluctuations produced by sudden accelerations. The further study of the changes in the occurrence of aftershocks led us to decompose the series into two type of events: leading aftershocks, accounting for the events that follow a relaxation law, and cascades for those events that do not. Finally, the series of cascades was characterized by noting that they can be fitted with straight lines whose slopes obey another power law with an exponent of about 1.08. Actually, the exponent ν range between 1.00 and 1.08 depending on the conservation level π and the value of ρ.This appears to be a smooth dependence. Varying the value of ρ at constant dissipation, the exponent increases from 1.00 to 1.08 as ρ increases, whereas for fixed values of ρ the exponent decreases as the dissipation level increases. As a consequence, future efforts will be devoted to understanding the dynamical characteristics of the model and their particular dependence on ρ and π by studying another complex series of aftershocks.

Acknowledgments Y.M thanks the AECI for financial support. This work was supported in part by the Spanish DGYCYT.

References

Atkinson, B.K., Subcritical crack growth in geological materials, *J. Geophys. Res., B89*, 4077-114, 1984.

Atkinson, B.K., and P.G. Meredith, The theory of subcritical crack growth with application to minerals and rocks, In B.K. Atkinson (Ed), *Fracture Mechanics of Rocks* (Academic Press, London), 111-166, 1987.

Barnet R.L., and R. Kerrich, Stress corrosion cracking of biotite and feldspar, *Nature, 283*, 185-187, 1980.

Benioff, H., Earthquakes and rock creep, *Bull. Seism. Soc. Am., 41*, 31-62, 1951.

Bonn, D., H. Kellay, M. Prochnow, K. Ben-Djemiaa, and J. Meunier, Delayed fracture of an inhomogeneous soft solid, *Science, 280*, 265-267, 1998.

Brace, W.F., and J.D. Byerlee, Stick-slip as a mechanism of earthquakes, *Science, 153*, 990-992, 1966.

Burridge, R., and Knopoff, L., Model and theoretical seismicity, *Bull. Seism. Soc. Am., 57*, 341-371, 1967.

Conchard, A., and R. Madariaga, Complexity of seismicity due to highly rate-dependent friction, *J. Geophys. Res., B101*, 25321-36, 1996.

Coleman, B.D., Time dependence of mechanical breakdown in bundles of fibers, *J. Appl. Phys. 28*, 1058, 1957.

Coleman, B.D., Time dependence of mechanical breakdown in bundles of fibers, III: The power law breaking rule, *Trans. Soc. Rheology, 2*, 195-218, 1958.

Correig, A.M., M. Urquizú, J. Vila, and S. Manrubia, Aftershock series of event February 18, 1996: An interpretation in terms of self-organized criticality, *J. Geophys. Res., B102*, 27,407- 20, 1997.

Daniels, H.E., The statistical theory of the strength of bundles of threads *Proc. Roy. Soc. Lond. A183*, 404, 1945.

Das, S., and C.H. Scholz, Theory of time-dependent rupture in the earth, *J. Geophys. Res., B86*, 6039-51, 1981.

Deuerler, F., R. Knehans, and R. Steinbrech, *Fortsch. deutschen Keram. Gess., 1*, 51, 1985.

Dieterich, J.H., Time-dependent friction in rocks, *J. Geophys. Res., 77*, 3690-97, 1972a.

Dieterich, J.H., Time-dependent friction as a possible mechanism for aftershocks, *J. Geophys. Res., 77*, 3771-81, 1972b.

Dieterich, J.H., Modeling of rock friction, 1, Experimental results and constitutive equations, *J. Geophys. Res., B84*, 2161-68, 1979.

Dieterich, J.H., A constitutive law for rate of earthquake production and its application to earthquake clustering, *J. Geophys. Res., B99*, 2601-18, 1994.

Garcimartín, A., A. Guarino, L. Bellon, and S. Ciliberto, Statistical properties of fracture precursors, *Phys. Rev. Lett., 79*, 17, 3202-05, 1997.

Gómez, J.B., Y. Moreno, and A.F. Pacheco, Probabilistic approach to time-dependent load-tranfer models of fracture, *Phys. Rev. E58*, 1528-32, 1998.

Gu, J.C., J.R. Rice, A.L. Ruina, and S.T. Tse, Slip motion and stability of a single degree of freedom elastic system with rate and state dependent friction, *J. Mech. Phys. Solids, 32*, 167-196, 1984.

Heaton, T.H., Evidence for and implications of self-healing pulses of slip in earthquake rupture, *Phys. Earth Planet. Inter., 64*, 1-20, 1990.

Hirata, T., Omori's power law aftershock sequences of microfracturing in rock fracture experiments, *J. Geophys. Res., B92*, 6215-21, 1987.

Kostrov, B.V., L.V. Nikitin, and L.M. Flitman, The mechanics of brittle fracture, *Mech. Solids, 3*, 105-117, 1969.

Lee, M.W., *Unstable fault interactions and earthquake self-organization*, PhD Thesis, UCLA, 1999.

Lee, M.W., and D. Sornette, Novel mechanism for discrete scale invariance in sandpile models, *cond-mat/9903402*, 27 Mar 1999.

Lockner, D., The role of acoustic emission in the study of rock, *Int. J. Rock Mech. Min. Sci. & Geomech. Abstr., 30*, 883-899, 1993.

Lockner, D., and Byerlee, J.D., Acoustic emission and creep in rocks at high confining pressures and differential stress, *Bull. Seism. Soc. Am., 67*, 247-258, 1977.

Marcellini, A., Arrhenius behavior of aftershock sequences, *J. Geophys. Res., B100*, 6463-68, 1995.

Marcellini, A., Physical model of aftershock temporal behavior, *Tectonophysics, 277*, 137- 146, 1997.

Newman, W.I., D.L. Turcotte, and A.M. Gabrielov, Log-periodic behavior of a hierarchical failure model with applications to precursory sesimic activation, *Phys. Rev. E52*, 4827-35, 1995.

Ogata, Y., Statistical models for earthquake occurrence and residual analysis for point processes, *J. Am. Stat. Assoc., 83*, 9-27, 1988.

Okoroafor, E.U., and R. Hill, Investigations of complex failure modes in fibre bundles during dynamic mechanical testing using acoustic emission and Weibull statistics, *J. Materials Sci., 30*, 4233-43, 1995.

Omori, F, On after-shocks of earthquakes, *J. Coll. Sci. Imp. Univ. Tokyo, 7*, 111-200, 1894.

Pauchard, L, and J. Meunier, Instantaneous and time-lag breaking of a two-dimensional solid rod under a bending stress, *Phys. Rev. Lett., 70*, 23, 3565-68, 1993.

Phoenix, S.L., Stochastic strength and fatigue in fiber bundles, *Int. J. Fracture, 14*, 327-344, 1977.

Phoenix, S.L., and L. Tierney, A statistical model for the time dependent failure of unidirectional compositie materials under local elastic load-sharing among fibers, *Eng. Frature Mech., 18*, 193-215, 1983.

Rice, J.R., and A.L. Ruina, Stability of steady frictional slipping, *J. Appl. Mech., 50*, 343-349, 1983.

Rice, J.R., and S.T. Tse, Dynamic motion of a single degree-of-freedom system following a rate- and state-dependent friction law, *J. Geophys. Res., B91*, 521-530, 1986.

Rigo, A., C. Olivera, A. Sourian, S. Figueras, H. Paucher, A. Grésillaud, and M. Nicolas, The February 1996 earthquake sequence in the eastern Pyrenees: first results, *J. Seismology, 1*, 3-14, 1997.

Ruina, A.L., Slip instability and state variable friction laws, *J. Geophys. Res., B88*, 10,359-70, 1983.

Sammonds, P.R., P.G. Meredith, and I.G. Main, Role of pore fluids in the generation of sesimic precursors to shear fracture, *Nature, 359*, 228-230, 1992.

Scholz, C.H., The frequency-magnitude relation of microfracturing in rock and its relation to earthquakes, *Bull. Seismol. Soc. Am., 58*, 399-415, 1968a.

Scholz, C.H., Microfractures, aftershocks, and seismicity, *Bull. Seismol. Soc. Am., 58*, 1117- 30, 1968b.

Scholz, C.H., *The Mechanics of Earthquakes and Faulting*, Cambridge University Press, New York, USA, 1990.

Utsu, T., A statistical study on the occurrence of aftershocks, *Geophys. Mag., 30*, 521-605, 1961.

Utsu, T, Y. Ogata, and S Matsu'ura, The centenary of the Omori formula for a decay law of aftershock activity, *J. Phys. Earth, 43*, 1-33, 1995.

Vazquez-Prada, M, J.B. Gómez, Y. Moreno, and A.F. Pacheco, Time to failure of hierarchical load-transfer models of fracture, *Phys. Rev. E*, in press, 1999.

Wennerberg, L., and Sharp, R.V., Bulk-friction of afterslip and the modified Omori law, *Tectonophysics, 277*, 109-136, 1997.

Wiederhorn, S.M., Influence of water vapor on crack propagation in soda-lime glass, *J. Amer. Ceram. Soc, 50*, 407-418, 1967.

Williams, D.P., *Int. J. Fracture, 9*, 63, 1973.

Yamashita, T, and L. Knopoff, Model of aftershock occurrence, *Geophys. J. R. Astron. Soc., 91*, 13-26, 1987.

Zhurkov, S.N., Kinetic concept of the strength of solids, *Int. J. Fracture Mech., 1*, 311-323, 1965.

This preprint was prepared with the AGU LaTeX macros v3.1. File JGRPAP22 formatted 1999 August 3.

Figure 1. Aftershock sequence of February 18, 1996, eastern Pyrenees. (a) Complete series of aftershocks, shown as the accumulated number of events (left axis), together with their magnitude (rigth axis, in relative units). (b) First 300 hours of the aftershock sequence, as used in the comparison with the model results. (c) Separation of the aftershock sequence into leading aftershocks (filled circles) and cascade events (dots). See the text for details.

Figure 2. (a) Series formed by the leading aftershocks, after removing from the original sequence the cascades. The fit to the Omori law is much better than the original, and the p value (0.94) is also closer to worldwide aftershock p-values. (b) Cascades retrieved from the original first 300 hours of the aftershock sequence. Each cascade can be approximated by a straight line.

Figure 3. Slope of the cascades versus time. It can be clearly seen that that they follow a power law $s \propto t^{-\nu}$, with $\nu \approx 0.7$

Figure 4. Rate of aftershocks dN/dt as a function of dimensionless time for a dissipation of $\pi = 0.7$ and a Weibull index of $\rho = 30$. The spikes that decorate the general t^-1 trend correspond to sudden accelerations in event rate (avalanches). The diagonal straight line has a slope of 1.

Figure 5. Accumulated number of aftershocks N as a function of dimensionless time for a dissipation of $\pi = 0.7$ and a Weibull index of $\rho = 30$. Note the sudden increases in event rate (step-like jumps) superimposed to the general Omori-law trend.

Figure 6. (a) Leading aftershock sequence for a simulation with $\pi = 0.7$ and $\rho = 30$. (b)Model cascades. The first event in each cascade is a leading aftershock. Note that the cascades can be also approximated by straight lines, as was the case with the cascades in the actual aftershock sequence, Fig. 2.

Figure 7. (a) Slopes of the model cascades versus dimensionless time of the leading event that initiate each cascade. Only the first part of the model cascades is shown in this plot to facilitate comparison with Fig. 3. (b) Log-log representation of the slopes versus time for the long-time tail of the simulation. As for the eastern Pyrenees series of aftershocks, the slopes fit very well a power law, in this case with an exponent of about 1.08.

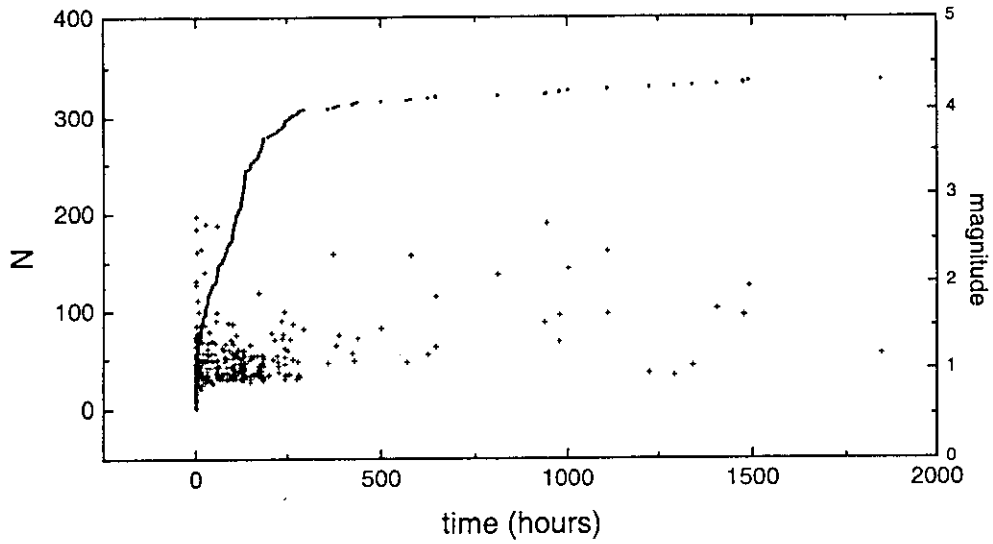
N
magnitude
time (hours)
0
100
200
300
400
0
1
2
3
4
5
0
500
1000
1500
2000

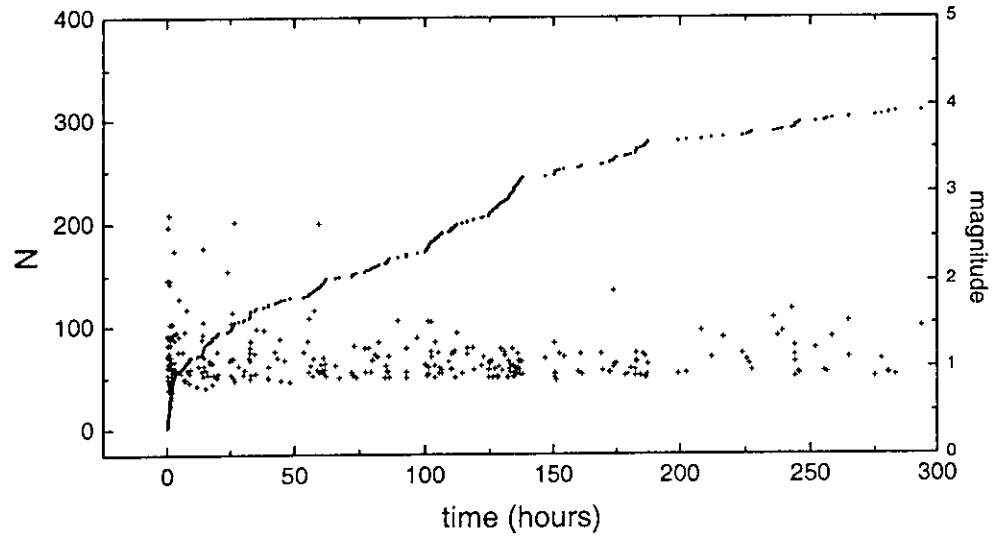
N
magnitude
time (hours)
0
100
200
300
400
0
1
2
3
4
5
0
50
100
150
200
250
300

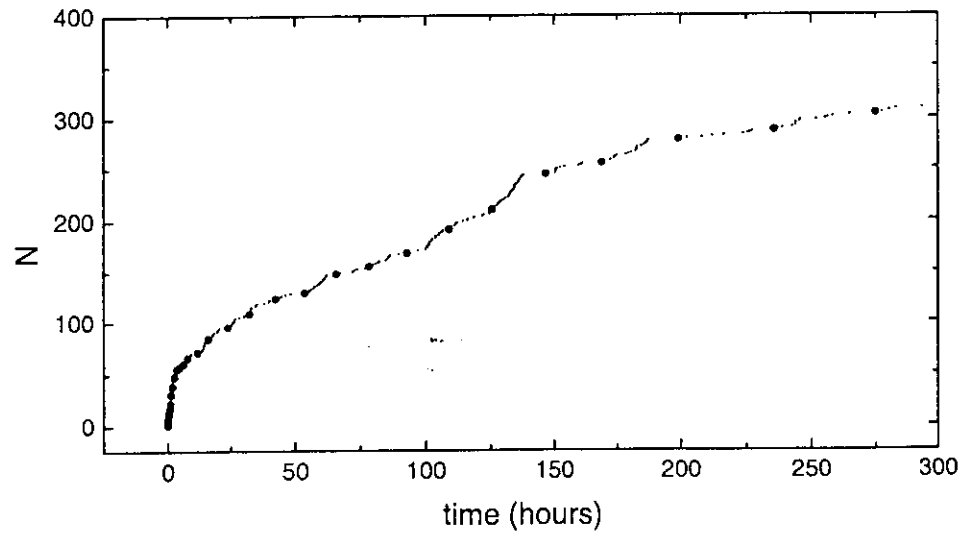
N
time (hours)
0
100
200
300
400
0
50
100
150
200
250
300

F 1

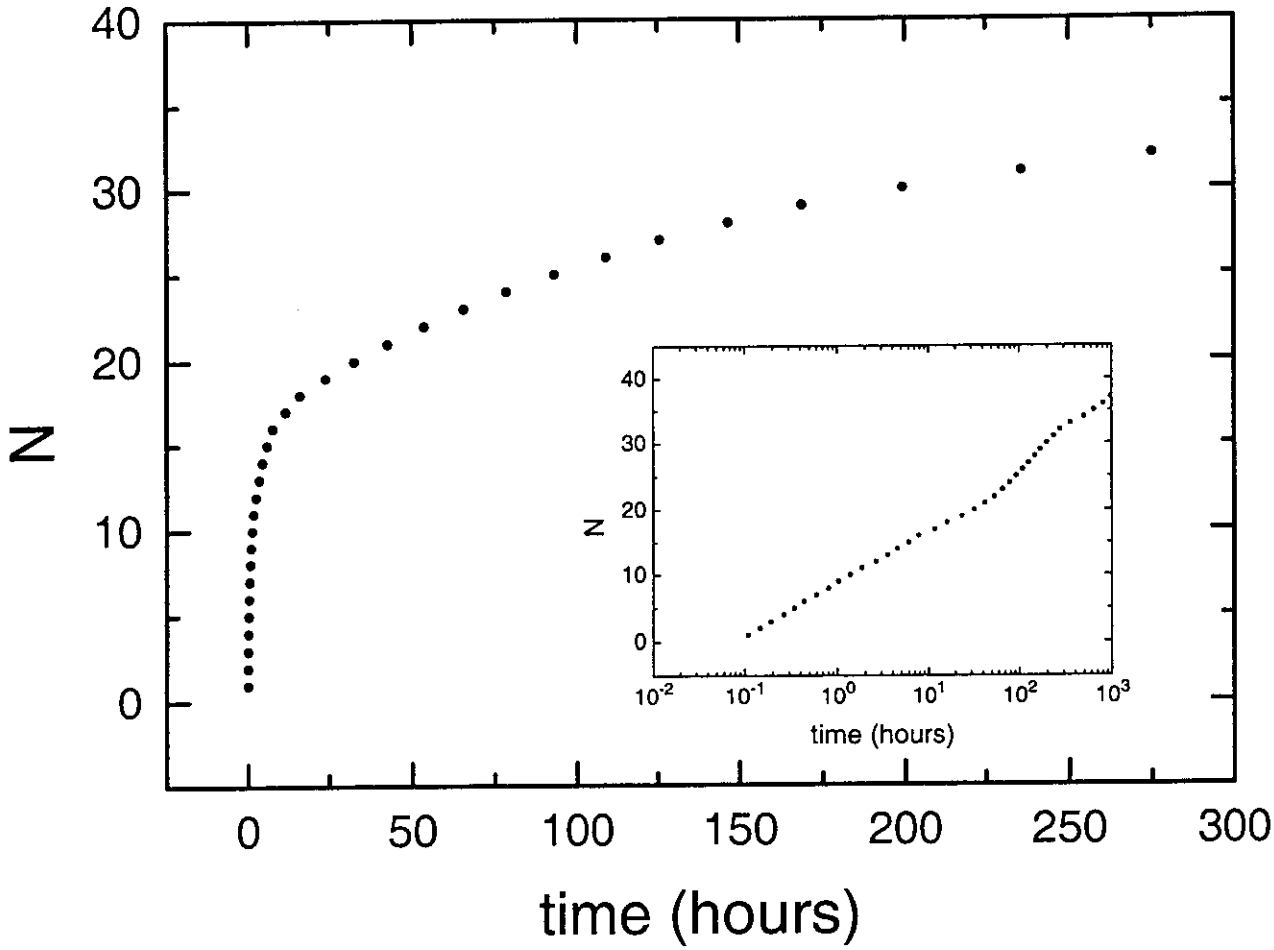
N
time (hours)
0
10
20
30
40
50
100
150
200
250
300
N
time (hours)
10^{-2}
10^{-1}
10^{0}
10^{1}
10^{2}
10^{3}

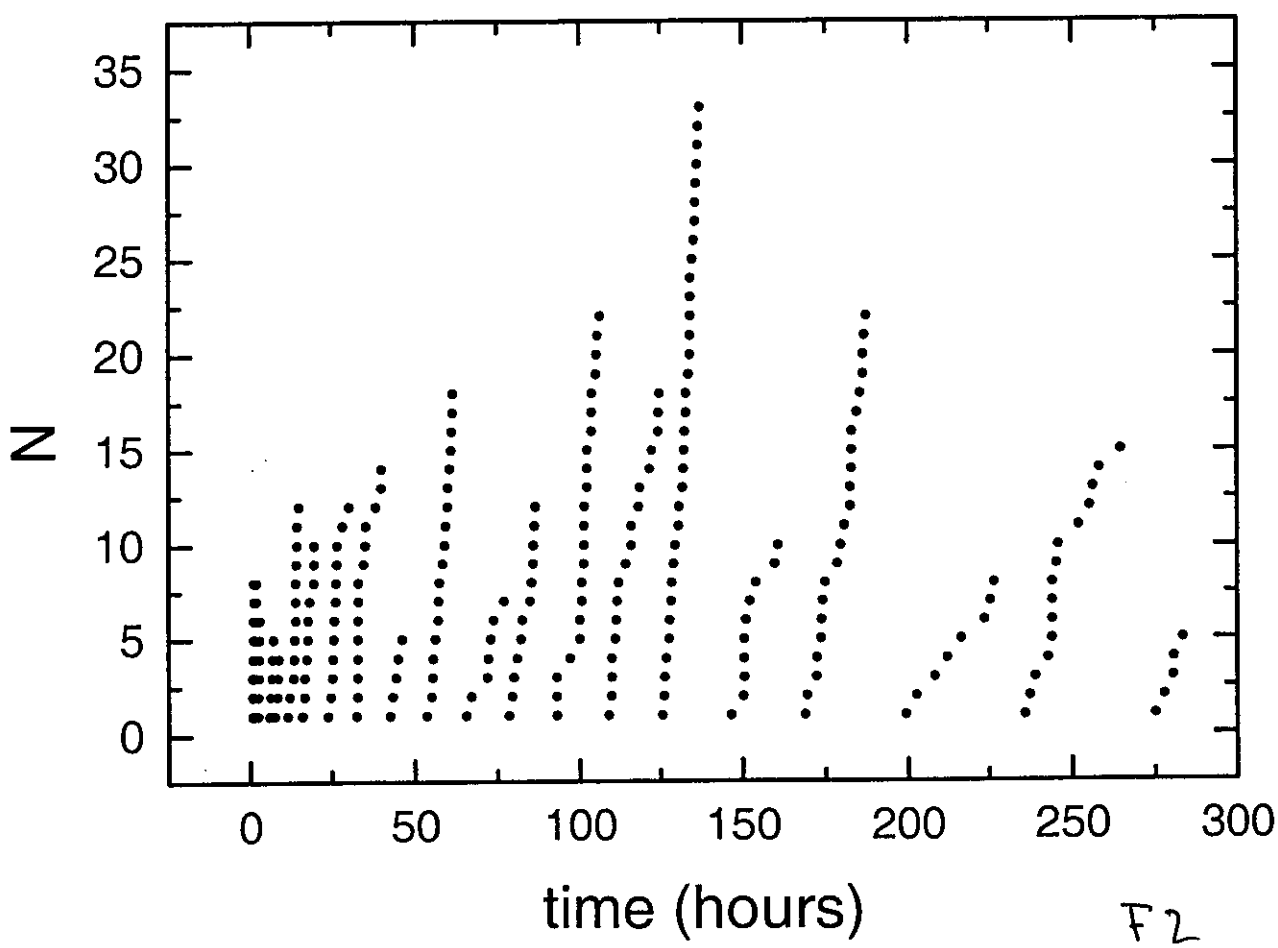
N
time (hours)
0
5
10
15
20
25
30
35
50
100
150
200
250
300

F2

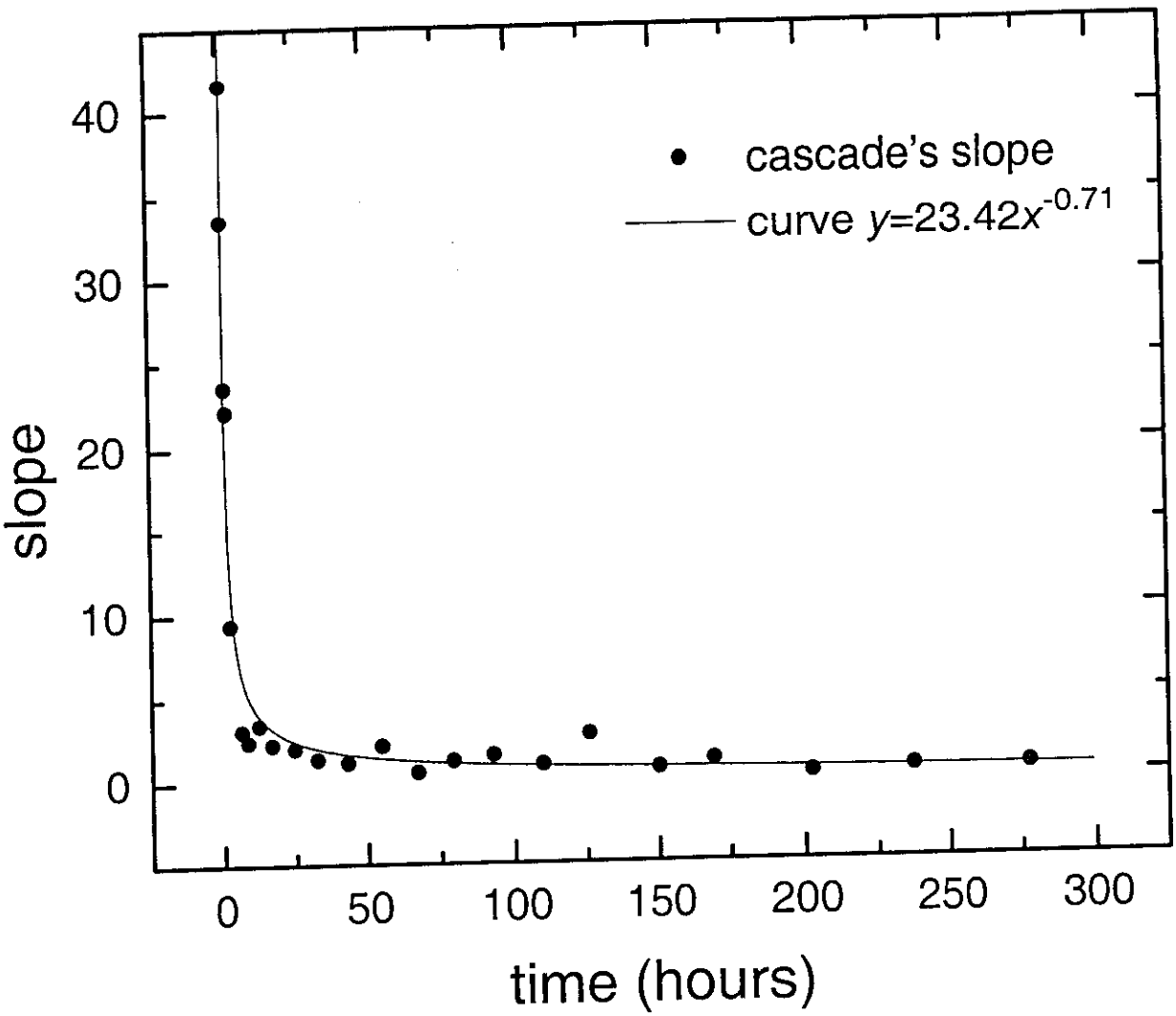
cascade's slope
curve $y=23.42x^{-0.71}$
slope
time (hours)
0
10
20
30
40
0
50
100
150
200
250
300

F 3

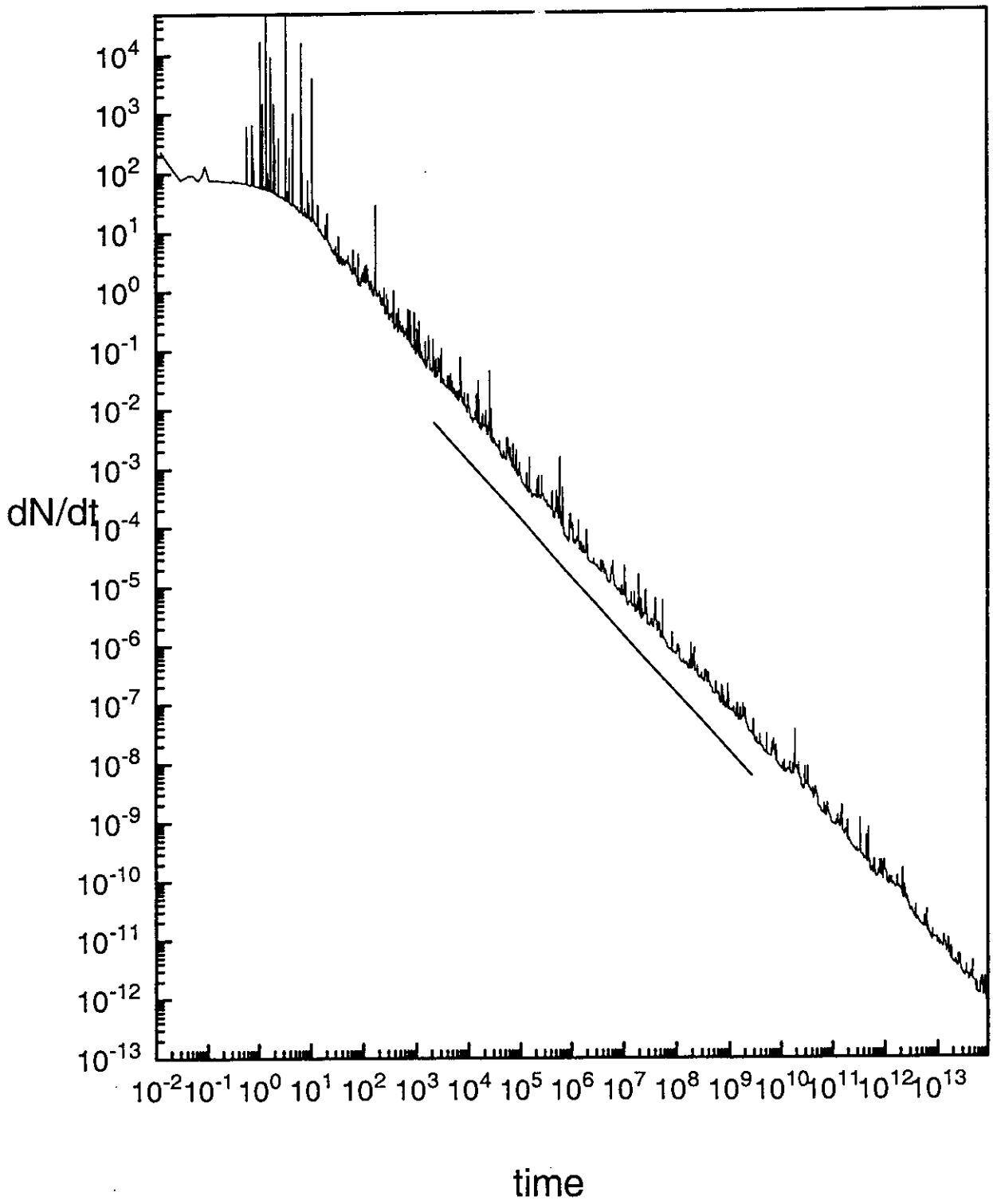
dN/dt
10^{4}
10^{3}
10^{2}
10^{1}
10^{0}
10^{-1}
10^{-2}
10^{-3}
10^{-4}
10^{-5}
10^{-6}
10^{-7}
10^{-8}
10^{-9}
10^{-10}
10^{-11}
10^{-12}
10^{-13}
10^{-2} 10^{-1} 10^{0} 10^{1} 10^{2} 10^{3} 10^{4} 10^{5} 10^{6} 10^{7} 10^{8} 10^{9} 10^{10} 10^{11} 10^{12} 10^{13}
time

F4

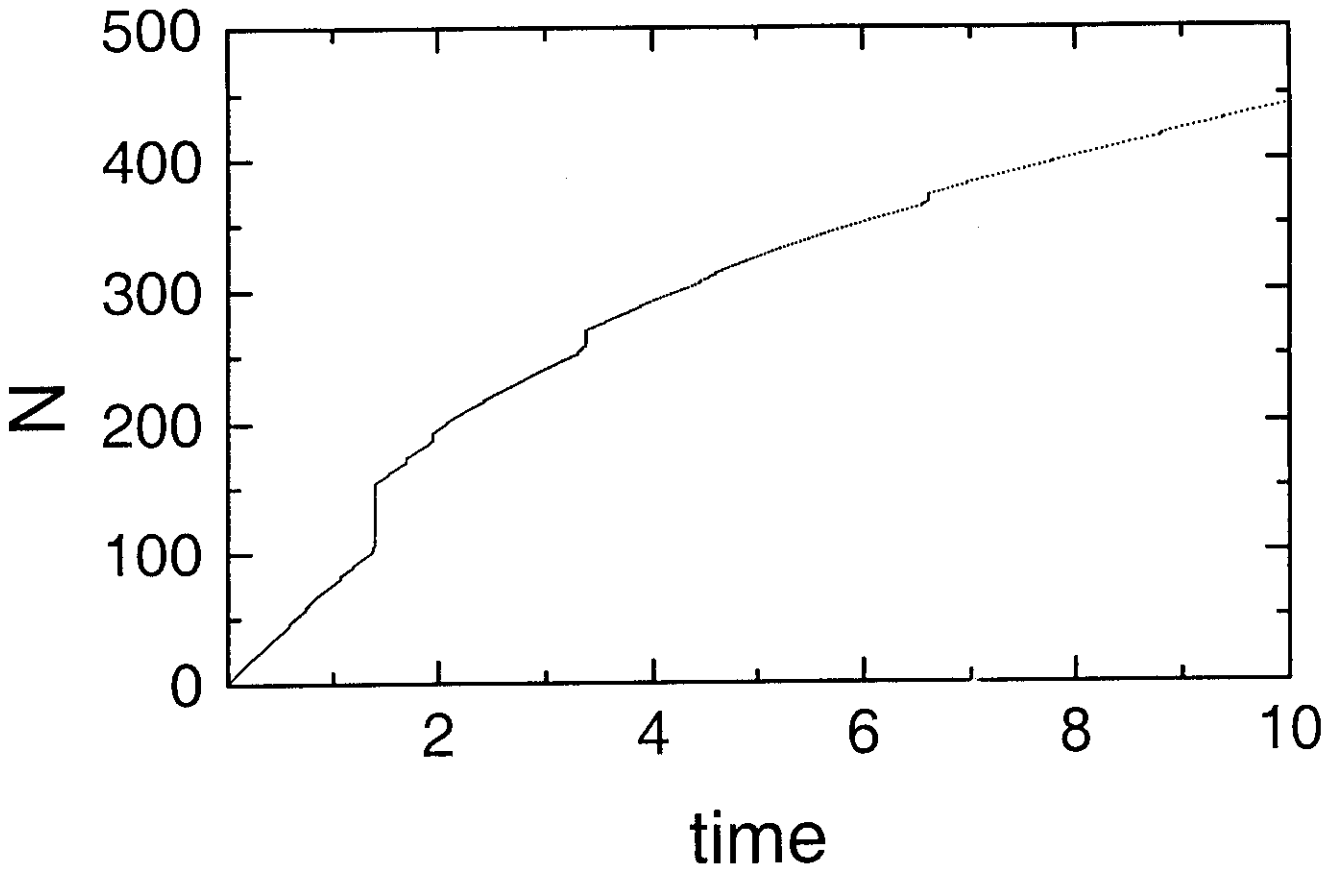

F5

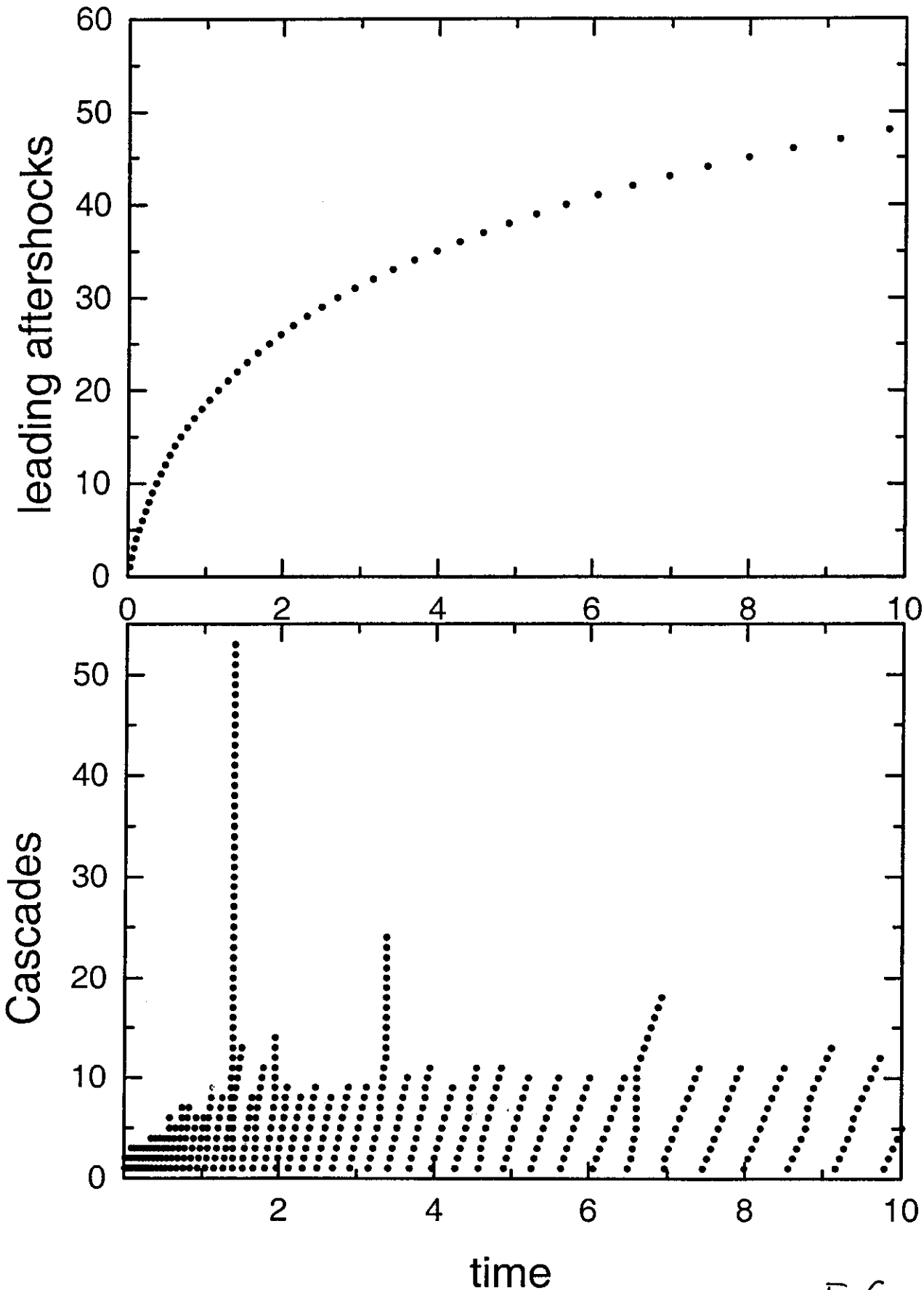
leading aftershocks
0
10
20
30
40
50
60
0
2
4
6
8
10
Cascades
0
10
20
30
40
50
2
4
6
8
10
time

F 6

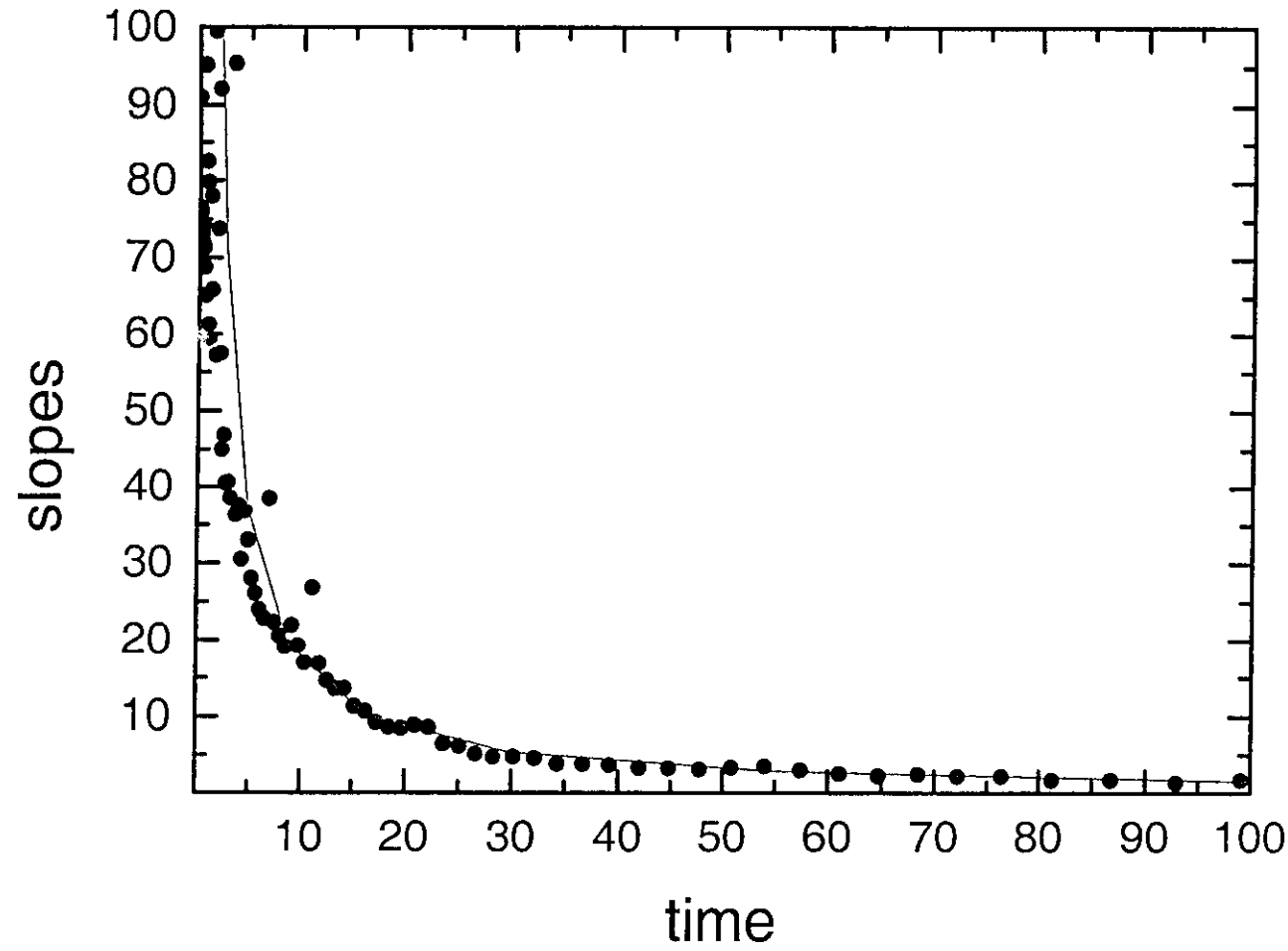
slopes
time
100
90
80
70
60
50
40
30
20
10
10 20 30 40 50 60 70 80 90 100

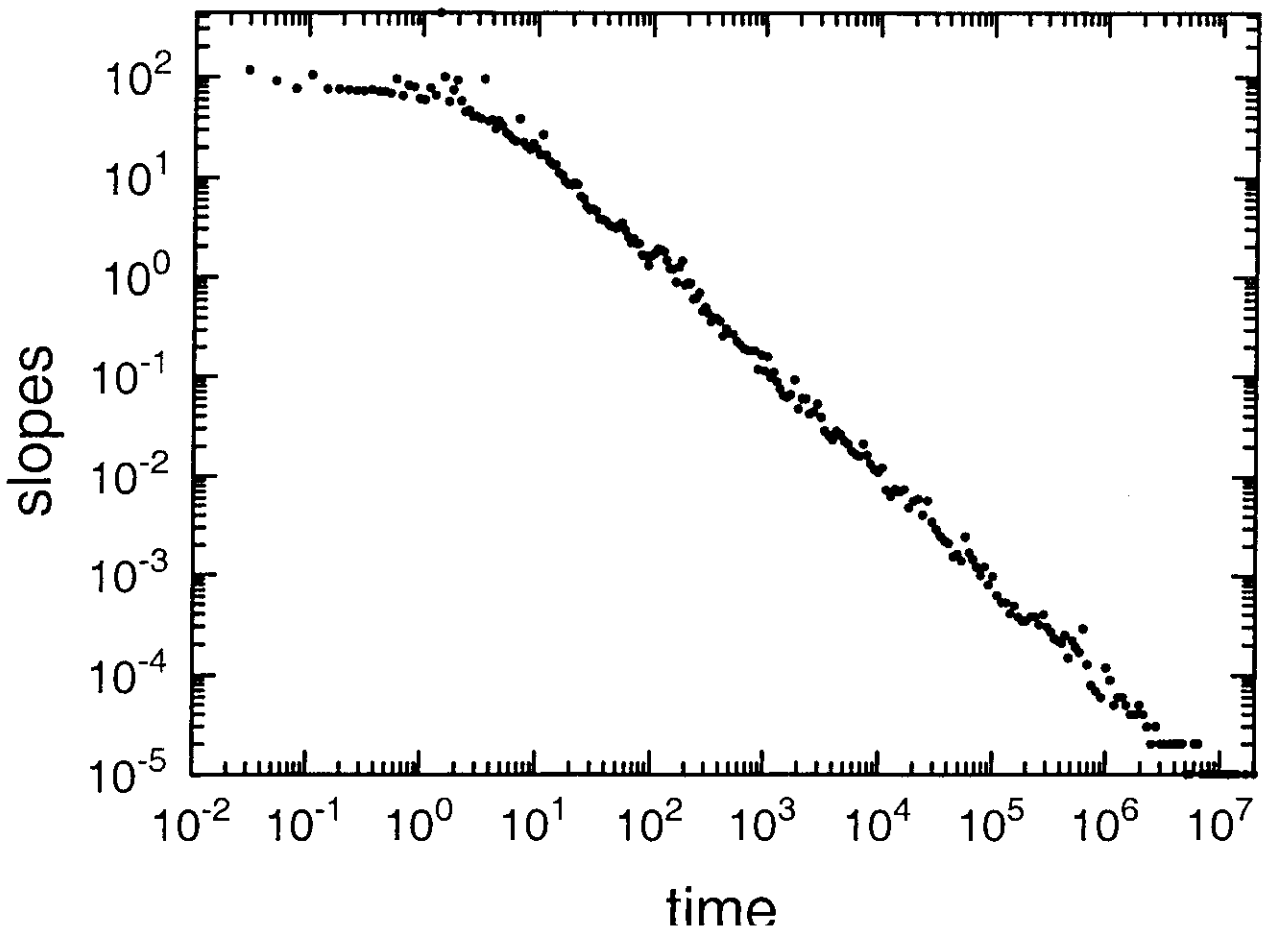
slopes
time
10^{2}
10^{1}
10^{0}
10^{-1}
10^{-2}
10^{-3}
10^{-4}
10^{-5}
10^{-2} 10^{-1} 10^{0} 10^{1} 10^{2} 10^{3} 10^{4} 10^{5} 10^{6} 10^{7}